ELSEVIER

Journal of Organometallic Chemistry 497 (1995) 133–142

Journal of Organometallic Chemistry

Addition of a sterically hindered, chiral crotyl *ansa*-titanocene complex to aldehydes ☆

Bradley A. Kuntz, Ravindranath Ramachandran, Nicholas J. Taylor, Jinying Guan, Scott Collins *

Department of Chemistry, University of Waterloo, Waterloo, Ontario N2L 3G1, Canada

Received 11 January 1995

Abstract

[*S*]-1,2-ethylenebis(3-t-butylcyclopendadienyl)titanium dichloride ([*S*]-**5**) can be obtained in high optical purity through kinetic resolution of the racemate (*rac*-**5**) using [*S*]-binaphthol. The structure of *rac*-1,2-ethylenebis(3-t-butylcyclopentadienyl)titanium binaphtholate (*rac*-**7**) was determined by X-ray crystallography: $C_{40}H_{40}O_2Ti$, monoclinic, $P2_1/c$, $a = 14.455(3)$ Å, $b = 13.710(3)$ Å, $c = 17.278(4)$ Å, $\beta = 109.80(2)$ °, $V = 3221.7(13)$ Å, $Z = 4$, 4599 observed reflections with $F \geq 6\sigma(F)$, $R = 0.0337$, $R_w = 0.0359$. The addition of [*S*] = (1-methylallyl)-1,2-ethylenebis(3-t-butylcyclopentadienyl)titanium ([*S*]-**6**), formed in situ from [*S*]-**5**, to aldehydes was investigated and provides β-methyl homoallylic alcohols in moderate yields. The stereoselectivity of the reaction and the sense of asymmetric induction depends on the steric bulk of the aldehyde. The results were rationalized using the results of a molecular modelling study on transition state models which reproduced the general trends in the experimental results.

Keywords: Titanium, *Ansa*-titanocene; Addition to aldehydes

1. Introduction

The addition of allyl organometallics to aldehydes has proven to be a useful method for the linear synthesis of polyacetate and polypropionate natural products [1]. High levels of diastereo- and enantioselectivity are possible when chiral type I or III allyl organometallics [2] react with aldehydes.

Bis(cyclopentadienyl)titanium(III) allyl complexes (**1**) [3] are type III allyl organometallics which add to aldehydes to furnish homoallylic alcohols **2** in high yields and, when substituted at C1 of the allyl group, with high simple diastereoselectivity for anti-**2** (Eq. (1) [4]. The diastereoselectivity of the reaction increases with increased steric bulk of both the aldehyde [4,5] and titanocene [5] substituents. These results have led to the hypothesis that the addition of the allyl group to the aldehyde occurs via a cyclic six-membered transition state [2,4,5]. The stereochemical results have been interpreted to indicate that a chair-like transition state is energetically favoured [4,5].

However, attempts to induce asymmetry in the organic products by use of chiral allyltitanocene compounds based on **1** have so far met with limited success [6–8]. Several years ago we investigated whether chiral, *ansa*-titanocene allyls might be useful in promoting enantioselective homoallylic alcohol formation [7]. Chiral allyltitanocenes [*S*]-**3a** and [*S*]-**3b** derived from *ansa*-titanocene dichloride [*S*]-**4** [9] reacted efficiently with aliphatic and aromatic aldehydes but, the addition proceeded with variable simple diastereoselectivity and poor to modest enantioselectivity (Eq. (2)).

The trends in stereoselectivity that were observed could not be uniformly rationalized in terms of chair-like transition states involving the chiral metallocene. In particular, the low simple diastereoselectivity observed

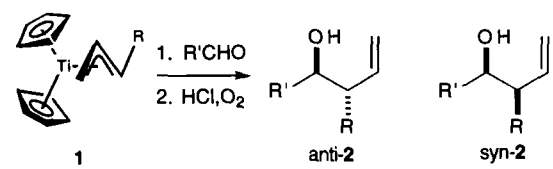

1 anti-2 syn-2 (1)

☆ Dedicated to Professor Hans-H. Brintzinger on the occasion of his 60th birthday.

* Corresponding author.

SSDI 0022-328X(95)00105-0

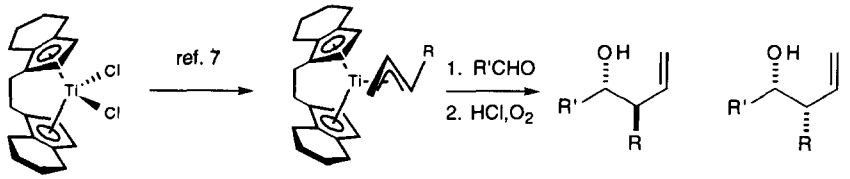

(2)

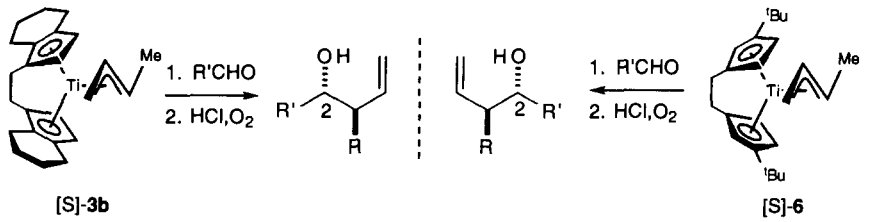

(3)

in the reactions of [*S*]-**3b** with sterically less hindered, aliphatic aldehydes seemed to suggest that twist-boat-like transition states might be of comparable energy. Moreover, the trends in enantioselectivity observed with reagents [*S*]-**3a** or [*S*]-**3b** and aldehydes were opposite; with reagent [*S*]-**3a**, sterically unhindered aldehydes provided homoallylic alcohols of the highest optical purity, whereas the converse was true using reagent [*S*]-**3b**, even though the sense of asymmetric induction using both reagents was the same.

Even with these incongruities, it seemed worthwhile to investigate the use of more sterically demanding ansa-titanocene complexes in this process; the magnitude of the asymmetric induction was expected to be improved based on simple models for the origin of enantioselectivity in these reactions. In this paper we disclose the preparation of optically pure, ansa-titanocene dichloride [*S*]-**5**, (obtained by kinetic resolution of the racemate), and the results of the reactions of allyltitanocene [*S*]-**6**, derived from [*S*]-**5**, with aldehydes.

2. Results

2.1. Resolution of complex rac-5

The efficient kinetic resolution of *rac*-**4** using [*S*] or [*R*]-binaphthol made this an obvious approach for obtaining optically pure, ansa-titanocene complex [*S*]-**5** [7,9b].

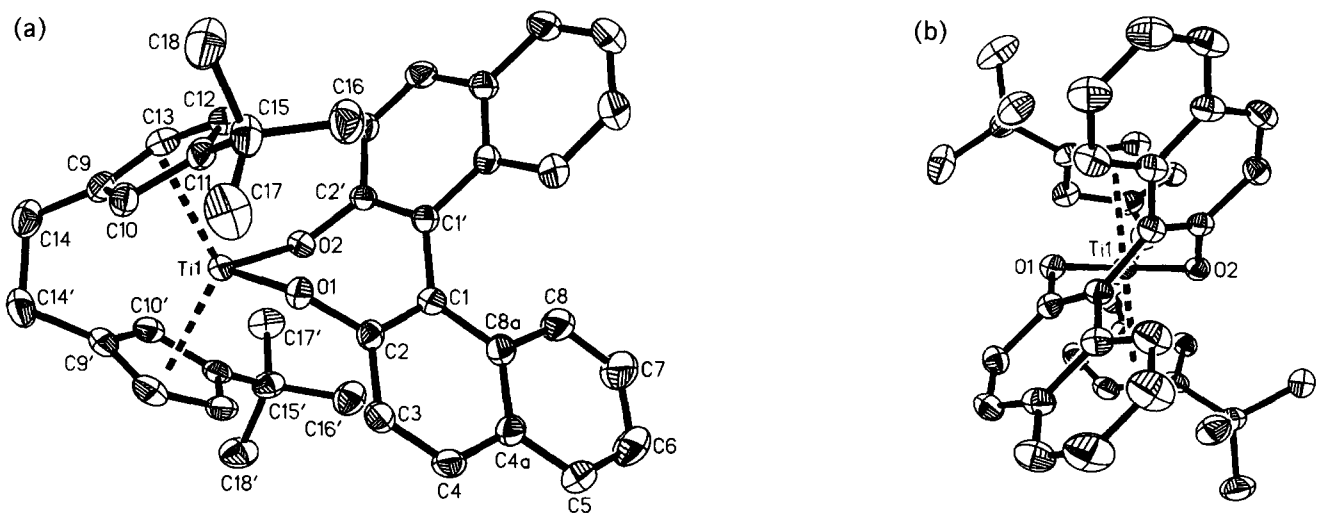

Fig. 1. Molecular structure of *rac*-**7** with 50% probability thermal ellipsoids depicted: (a) projection of the [*R*,*R*]-enantiomorph with atom-numbering scheme; (b) projection aligned with the bisector of the O1–Ti–O2 angle.

The reaction of *rac*-binaphthol with *rac*-**5** [10a] was highly stereoselective; reaction of *rac*-**5** with one equivalent of *rac*-binaphthol under optimized conditions (finely divided Na metal in toluene at 80°C—see Experimental Section for details) provided a 53% yield of a single, binaphtholate complex, *rac*-**7**. The yield is significantly lower than that obtained for the corresponding reaction of *rac*-**4** with *rac*-binaphthol under similar conditions (> 80% yield) [7,9b]. Presumably, the steric demands imposed by the *t*-butyl substituents in *rac*-**5** prevent rapid derivatization/cyclization and thus, reductive degradation of *rac*-**5** is competitive—indeed, very little of *rac*-**5** could be recovered from these reactions.

The X-ray structure of complex *rac*-**7** is depicted in Fig. 1(a), while an alternate projection, which clearly illustrates the complementary fit of the *ansa*-ligand to the binaphtholate ligand is shown in Fig. 1(b). Crystallographic data, atomic coordinates and selected bond lengths and angles appear in Tables 1–3. The structure is unexceptional with regard to the metal–centroid and metal–oxygen distances and exhibits approximate C_2 symmetry in the solid-state. The O1–Ti–O2 angle of 92.9 (1) ° is somewhat contracted from the normal values; this probably reflects the rather precise bite requirements of the binaphtholate ligand. The *ansa*-ligand framework has adopted the λ conformation [9a,10b] in this structure presumably, so as to mitigate severe repulsion between the *t*-butyl substituents and the binaphtholate ligand that would exist in the more commonly encountered, δ conformer [9a,10a]. As far as we are aware, *rac*-**7** is only the second, *ansa*-metallo-

Table 1
Crystallographic and refinement data for *rac*-**7**

Formula	$C_{40}H_{40}TiO_2$
MW	600.6
Crystal size (mm)	0.54{100}×0.48{010}×0.50{001}
Crystal system	Monoclinic
Cell constants	
a (Å)	14.455 (3)
b (Å)	13.710 (3)
c (Å)	17.278 (4)
β (°)	109.80 (2)
Volume (Å^3)	3221.7 (13)
Space group	$P2_1/c$
Z	4
ρ_{calc} (g cm^{-3})	1.238
Absorption coeff. (cm^{-1})	2.99
F(000)	1272
Diffractometer	Siemens R3m/V
Radiation	MoKα (λ = 0.71073 Å)
T (K)	200
Scan method	ω
Scan speed (° min^{-1})	2.93–29.30
Scan width (°)	1.2
2θ range (°)	3.5–50
Unique data	5676
Observed data ($F \geq 6\sigma(F)$)	4599
Absorption corr.	Face-indexed analytical
Transmission factors	0.816–0.892
Structure solution	Patterson and Fourier
Structure refinement	Full-Matrix Least-Squares
Extinction corr.	$\chi = 0.000147(8)$
Hydrogen atoms	Refined isotropic U
Weighting scheme	$w^{-1} = \sigma^2(F)$
R	0.0337
R_w	0.0359
GOF	2.65
Data-to-parameter ratio	8.4:1
Max. residuals (e Å^{-3})	0.26, −0.30

Table 2
Atomic coordinates (×10^4) and equivalent isotropic displacement coefficients (Å^2 ×10^3)

	x	*y*	*z*	U_{eq} [a]
Ti(1)	2619.0(3)	579.8(3)	1236.2(2)	21.0(1)
O(1)	3545(1)	16(1)	2195.0(8)	24.2(5)
O(2)	1516(1)	57(1)	1477.4(8)	23.3(5)
C(1)	2739(1)	−597(2)	3097(1)	23.9(7)
C(2)	3450(1)	−16(1)	2945(1)	22.5(7)
C(3)	4126(2)	533(2)	3587(1)	26.0(7)
C(4)	4066(2)	546(2)	4354(1)	28.2(8)
C(4A)	3327(2)	16(2)	4536(1)	28.0(8)
C(5)	3240(2)	40(2)	5328(1)	39(1)
C(6)	2521(2)	−457(2)	5499(2)	51(1)
C(7)	1835(2)	−1005(2)	4874(2)	50(1)
C(8)	1902(2)	−1047(2)	4101(2)	38(1)
C(8A)	2652(2)	−557(2)	3902(1)	27.5(8)
C(1′)	2078(2)	−1247(2)	2447(1)	23.5(7)
C(2′)	1467(1)	−881(1)	1697(1)	22.4(7)
C(3′)	755(2)	−1490(2)	1136(1)	27.2(8)
C(4′)	717(2)	−2460(2)	1281(1)	30.6(8)
C(4A′)	1391(2)	−2893(2)	1993(1)	28.8(8)
C(5′)	1410(2)	−3915(2)	2130(2)	38(1)
C(6′)	2083(2)	−4322(2)	2810(2)	44(1)
C(7′)	2773(2)	−3728(2)	3382(2)	40(1)
C(8A′)	2075(2)	−2281(2)	2580(1)	26.2(8)
C(8′)	2770(2)	−2740(2)	3272(1)	32.9(9)
C(9)	2704(2)	555(2)	−119(1)	28.2(8)
C(10)	3643(2)	240(2)	415(1)	27.3(8)
C(11)	3541(2)	−698(2)	723(1)	25.8(8)
C(12)	2538(2)	−919(2)	426(1)	27.2(8)
C(13)	2025(2)	−158(2)	−85(1)	28.9(8)
C(14)	2501(2)	1490(2)	−604(1)	35.4(9)
C(15)	4377(2)	−1373(2)	1195(1)	32.6(8)
C(16)	4079(2)	−2074(2)	1757(2)	39(1)
C(17)	5294(2)	−807(2)	1683(2)	48(1)
C(18)	4598(3)	−1999(2)	530(2)	51(1)
C(9′)	2689(2)	2214(2)	747(1)	28.6(8)
C(10′)	1738(2)	2099(2)	789(1)	26.3(8)
C(11′)	1798(2)	2031(1)	1621(1)	25.2(7)
C(12′)	2801(2)	2030(2)	2089(1)	27.2(8)
C(13′)	3351(2)	2138(2)	1562(1)	30.7(8)
C(14′)	2939(2)	2340(2)	−22(2)	37(1)
C(15′)	945(2)	2090(2)	1951(1)	30.0(8)
C(16′)	1170(2)	1536(2)	2765(2)	38(1)
C(17′)	−18(2)	1714(2)	1331(2)	37(1)
C(18′)	827(2)	3184(2)	2106(2)	43(1)

[a] Equivalent isotropic *U* defined as one-third of the trace of the orthogonalized U_{ij} tensor.

Table 3
Selected bond lengths and angles for *rac*-**7** [a]

Bond lengths (Å)			
Ti–O(1)	1.906(1)	Ti–O(2)	1.918(2)
Ti–Cn [b]	2.123(2)	Ti–Cn' [b]	2.116(2)
Ti–C(9)	2.390(2)	Ti–C(9')	2.404(2)
Ti–C(10)	2.420(3)	Ti–C(10')	2.431(2)
Ti–C(11)	2.536(2)	Ti–C(11')	2.517(2)
Ti–C(12)	2.470(2)	Ti–C(12')	2.435(2)
Ti–C(13)	2.377(2)	Ti–C(13')	2.366(2)
Bond angles (°)			
O(1)–Ti–O(2)	92.8(1)	Cn–Ti–Cn' [b]	128.7(1)
Ti–O(1)–C(2)	125.4(1)	Ti–O(2)–C(2')	122.9(1)
O(1)–C(2)–C(1)	121.3(2)	O(2)–C(2')–C(1')	121.9(2)
C(2)–C(1)–C(1')	121.4(2)	C(2')–C(1')–C(1)	122.0(2)
O(1)–Ti–C(9)	126.3(1)	O(2)–Ti–C(9')	124.2(1)
O(1)–Ti–C(10)	92.4(1)	O(2)–Ti–C(10')	90.3(1)
O(1)–Ti–C(11)	74.0(1)	O(2)–Ti–C(11')	74.7(1)
O(1)–Ti–C(12)	92.3(1)	O(2)–Ti–C(12')	95.8(1)
O(1)–Ti–C(13)	125.7(1)	O(2)–Ti–C(13')	128.7(1)
O(1)–Ti–C(9')	125.6(1)	O(2)–Ti–C(9)	122.3(1)
O(1)–Ti–C(10')	139.8(1)	O(2)–Ti–C(10)	140.9(1)
O(1)–Ti–C(11')	110.3(1)	O(2)–Ti–C(11)	112.9(1)
O(1)–Ti–C(12')	84.5(1)	O(2)–Ti–C(12)	85.9(1)
O(1)–Ti–C(13')	91.9(1)	O(2)–Ti–C(13)	89.6(1)

[a] Bond lengths and angles with estimated standard deviation in parentheses. For the atom numbering scheme, consult Fig. 1.
[b] Cn and Cn' are the two centroids of the cyclopentadienyl rings.

cene binaphtholate complex to be structurally characterized [9b].

Kinetic resolution of *rac*-**5** with 0.5 equivalents of [*S*]-binaphthol, under the same conditions, provided enantiomerically pure [*S,S*]-**7** (53% yield based on one enantiomer, Scheme 1). This material could be converted to optically pure [*S*]-**5** by reaction with methyllithium in ether-hexane solution followed by filtration of the insoluble, binaphtholate salt and treatment of the filtrate with a solution of anhydrous HCl in ether. Compound [*S*]-**5** is an extremely soluble material compared with its racemate (in agreement with earlier findings [9b] and was obtained in 90–95% yields from [*S,S*]-**7**.

The optical purity of [*S*]-**5** was indirectly determined by reaction of the intermediate, dimethyl-titanocene [*S*]-**8** with 2 equiv. of [*S*]-O-acetylmandelic acid in $CDCl_3$ [9a]. The chemical shifts for both diastereomers [*R,S,S*]-**9** and [*S,S,S*]-**10** (which were prepared from *rac*-**5** via *rac*-**8**), are collected in Table 4. As the resonances for the [*R,S,S*]-**9** were not present in the 200 MHz ^{1}H NMR spectrum of the material derived from [*S*]-**8**, the optical purity of the latter material must be in excess of 98% ee.

2.2. Reactions of [S]-6 with aldehydes

Reduction of [*S*]-**5** was accomplished by treatment with ^{n}PrMgBr in THF [3,7]. Subsequent transmetallation with crotylmagnesium chloride furnished solutions of [*S*]-**6**, which were deep purple in colour. The reactions of [*S*]-**6** with various aldehydes were investigated, and these results are depicted in Table 5. We also investigated the effect of changing solvent polarity on the efficiency and selectivity of these addition reactions. Preparation of [*S*]-**6**, by reduction of [*S*]-**5** with ^{n}PrMgBr in hexane suspension and subsequent transmetallation with crotylmagnesium chloride, also gave consistent results upon subsequent reaction with aldehydes (Table 5).

Table 4
Selected ^{1}H-NMR chemical shifts for bis-[*S*]-O-acetylmandelate derivatives of [*S*]-**8** [a]

[*R,S,S*]-**9**	[*S,S,S*]-**10**	Assignment
6.75	6.33	CpH (t, 2H)
6.16	6.05	CpH (t, 2H)
6.04	5.98	CpH (t, 2H)
5.80	5.97	$-O_2CH$(OAc)Ph (s, 2H)
2.20	2.15	–OAc (s, 6H)
0.68	0.71	$-C(CH_3)_3$ (s, 18H)

[a] Spectra were recorded in $CDCl_3$ solution at 200 MHz and 25°C; chemical shifts are referenced with respect to residual $CHCl_3$ at δ 7.26.

As can be appreciated from the results shown, the efficiency of the allylation reaction is variable; low to moderate yields of the homoallylic alcohols were obtained. In certain cases, the simple diastereoselectivity is very high (entries 1–4, 9–10) and this suggests that all of the crotylmagnesium chloride had been consumed prior to the addition of aldehyde [7]. The low yields may indicate that [*S*]-**6** reacts inefficiently with aldehydes, possibly due to the increase in steric hindrance at the metal centre in this complex.

Some of our earlier findings are mirrored in the results presented here [7]. Namely, the simple diastereoselectivity of the reaction (i.e. ratio of *anti*: *syn*) improves with the steric size of the aldehyde substituent and is essentially complete for benzaldehyde and pivaldehyde. This behaviour is expected for reactions involving a lower energy, chair-like transition state and η^1-crotylorganometallics with the more stable, *E*-configuration.

The use of [*S*]-**6** preferentially leads to the formation of the [*S*]-enantiomer of *anti*-**2** and the level of selectivity improves with the steric bulk of the aldehyde substituent (entries 5, 7, 1). However, for pivaldehyde there is a reversal in the sense of asymmetric induction (entry 9). Also, the *syn* stereoisomer of the homoallylic alcohol derived from phenylacetaldehyde was formed with greater enantioselectivity than the *anti* isomer (entry 5). Some of these trends are consistent with our earlier work but, with an important difference, the sense of asymmetric induction is *reversed* from that seen using

[*S*]-**3b** [7]. That is, the latter reagent provides *anti*-homoallylic alcohols of the [2*R*] configuration whereas, the use of [*S*]-**6** generally produces the [2*S*] enantiomer (Eq. (3)).

The temperature dependence of the enantioselectivity was investigated in one case and the enantioselectivity was found to improve dramatically on lowering the temperature, albeit at the expense of a diminution in the yield (entries 1–3). Finally, the polarity of the solvent has a minor effect on the stereoselectivity of this process under otherwise similar conditions (e.g. entries 1 and 4).

3. Discussion

The results obtained using [*S*]-**6** are intriguing and in certain cases, the level of enantio- and diastereo-selectivity is compelling (e.g. entry 3). Based on our earlier work, we had concluded that the favoured, chair-like, transition state using reagent [*S*]-**3b** was that which minimized steric repulsion between the tetrahydroindenyl ligand with the pseudo-axial aldehyde proton (i.e. **A'** lower in energy than **A**, Scheme 2 [7].

The fact that there is a reversal in the sense of asymmetric induction using the more sterically hindered [*S*]-**6** (i.e. **B** lower in energy **B'**, Scheme 2) strongly suggests that our earlier hypothesis is incorrect. A moment's reflection on this point will reveal that a very similar, but opposing, interaction will be experienced by the vinylic proton at the β-carbon of the crotyl ligand (Scheme 2). If this is of comparable magnitude to that of experienced by the aldehyde proton in the alternative, chair-like transition state, one expects no or low selectivity if these two interactions are crucial in determining stereochemistry. It is thus clear that the energy of interaction of the aldehyde with the crotyltitanocene complex is subtly influenced by both substitution on the aldehyde, the allyl substituent and the *ansa*-ligand in a manner which is *not* readily predicted using simple, transition state arguments.

In an attempt to rationalize the results observed with [*S*]-**6** (and [*S*]-**3b**), we have examined probable transition states in these allylation reactions by molecular modelling. Modelling of transition states by molecular mechanics has been a popular area of research in recent years. The most common approach has been to locate a transition state or state(s) for a simplified model system at the highest possible level of theory in order to obtain the force field parameters for the transition state [11]. This approach has been criticized since it can result in over-parameterization of the force field [12,13]. Menger and Sherrod have proposed that well chosen ground state analogues can act as models for the transition state [12]. Due to the large number of electrons present in the transition states of interest here, we have adopted a combination of these approaches.

The basic features of the transition state geometry for the forming C–C bond in these allylation reactions were

Table 5
Reactions of [*S*]-**6** with Aldehydes [a]

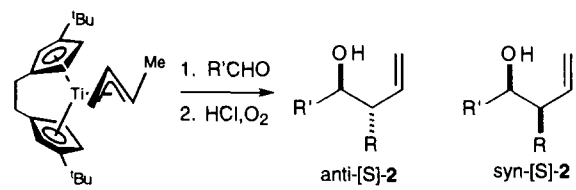

Entry	*R*	Solvent	*T* (°C)	Yield (%) [b]	anti-**2** : syn-**2** [c]	anti-[S] : [R]-**2** [c,d]
1	Ph	THF	25	50	> 99 : 1	4 : 1
2	Ph	THF	0	36	> 99 : 1	8 : 1
3	Ph	THF	−78	18	> 99 : 1	> 99 : 1
4	Ph	hexane	25	42	> 99 : 1	8 : 1
5	$PhCH_2$	THF	25	46	1.5 : 1	1.6 : 1 (1 : 5) [e]
6	$PhCH_2$	hexane	25	36	1.1 : 1	1.4 : 1 (1 : 5) [e]
7	c-C_6H_{11}	THF	25	64	10 : 1	3 : 1
8	c-C_6H_{11}	hexane	25	28	5 : 1	3 : 1
9	t-Bu	THF	25	34	> 99 : 1	1 : 3
10	t-Bu	hexane	25	50	> 99 : 1	1 : 3

[a] Complex [*S*]-**6** was generated in situ from [*S*]-**5** and 1.2 equiv. of *n*-PrMgCl (25–60°C), followed by treatment with 0.9 equiv. of crotylmagnesium chloride (25°C).
[b] Isolated yields following chromatography.
[c] Determined by ^1H NMR spectroscopy and/or by HPLC analysis of the 3,5-dinitrobenzoylcarbamate derivatives [7].
[d] In order to facilitate comparisons between aldehydes, the absolute configuration at the carbinol carbon of the homoallylic alcohols **2** is labeled according to the convention of Roush in which the aldehyde substituent is always assumed to have a higher priority than the crotyl group [21].
[e] The value in parentheses is the ratio of *syn*-[2*S*] : *syn*-[2*R*]-**2**.

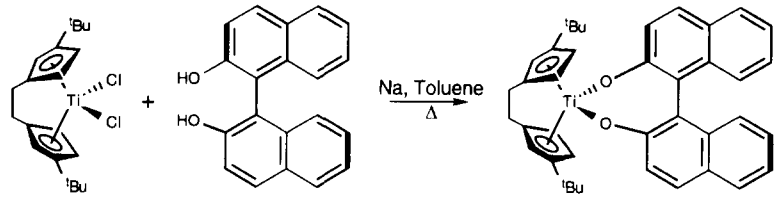

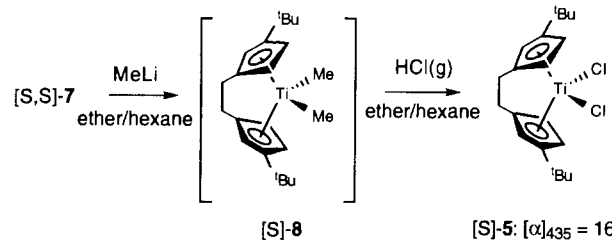

Scheme 1.

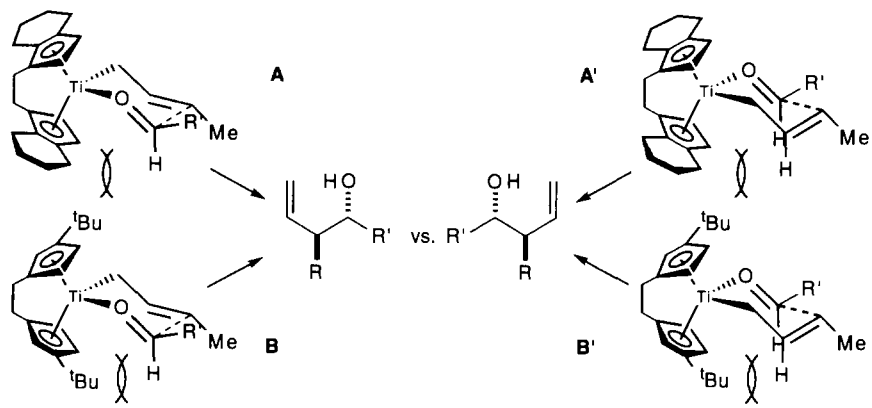

Scheme 2.

Table 6
MMX energies for chair-like transition states involving aldehydes and [*S*]-**6** and [*S*]-**3b** [a]

Reagent [*S*]-**6**						
R'CHO	[*S,S*]-**B** [b] (kcal mol^{-1})	[*S,R*]-**B'** [b] (kcal mol^{-1})	[*S,S*]-**B''** [c] (kcal mol^{-1})	ΔE [d] (kcal mol^{-1})	$\Delta E'$ [e] (kcal mol^{-1})	ΔE [f] (kcal mol^{-1})
$PhCH_2$	−35.1	−36.1	−38.3	1.0_0	2.2_3	0.28
c-C_6H_{11}	−57.8	−58.8	−60.5	1.0_4	1.7_6	0.65
^{t}Bu	−59.5	−60.5	−61.3	0.9_6	0.8_2	−0.65
Ph	−40.0	−41.5	−44.0	1.5_5	2.4_3	0.82
Reagent [*S*]-**3b**						
*R'*CHO	[*S,S*]-**A** [b] (kcal mol^{-1})	[*S,R*]-**A'** [b] (kcal mol^{-1})		ΔE [d] (kcal mol^{-1})		ΔE [f] (kcal mol^{-1})
$PhCH_2$	−30.7	−30.3		-0.4_6		−0.11
c-C_6H_{11}	−53.9	−54.5		0.5_4		0.41
^{t}Bu	−54.9	−56.1		1.2_0		0.74
Ph	−37.8	−37.6		-0.2_6		0.28

[a] All geometry optimizations were performed after VESCF calculations on the π atoms of the Cp rings were complete (default with PCMODEL).
[b] Refer to Scheme 2 for an idealized structure; in each case a C_2-symmetric conformation is adopted by *ansa*-ligand—see Fig. 2(a).
[c] Skewed conformation adopted by *ansa*-ligand—see text and e.g. Fig. 2(b).
[d] $\Delta E = E_{[S,S]\text{-B}} - E_{[S,R]\text{-B}'}$ (for [*S*]-**6**) or $E_{[S,S]\text{-A}} - E_{[S,R]\text{-A}'}$ (for [*S*]-**3b**).
[e] $\Delta E' = E_{[S,R]\text{-B}'} - E_{[S,S]\text{-B}''}$.
[f] Experimental values obtained at 25°C in THF solution.

expected to resemble those for the forming bond in a Cope rearrangement. Accordingly, the carbonyl carbon of the coordinated aldehyde and the γ-carbon of the crotyl ligand were assigned these atom types within the MMX force field and a fixed bond order of 0.3 (corresponding to an 'early' transition state) was adopted throughout. The carbonyl oxygen was assumed to develop alkoxide character in the transition state and was thus assigned as such and directly bonded to the titanium atom. The α and β-carbon atoms of the crotyl ligand were assigned parameters associated with sp^2-hybridized, carbon-centered radicals, reflecting the formation of a double bond between these two atoms in the transition state; the former carbon atom was coordinated to the metal. All other parameters were the standard ones employed within the software [14].

The x-ray structures of *rac*-**5** (which, in the space group $P42_1c$, assumes approximate C_2 symmetry) [10a] and *rac*-**4** [9b] were employed as a starting geometries but, all atoms were allowed to minimize—i.e. the only constraint was the fixed, bond-order between the C=O carbon and the γ-carbon of the crotyl ligand. The results of these calculations are summarized in Table 6 for chair-like transition states [15]. The negative MMX energies are a reflection of the large, attractive Van der Waal interactions, a common feature of MMX calculations involving cyclopentadienyl complexes.

Two, low energy, diastereomeric 'transition' states [*S*,*S*]-**B** and [*S*,*R*]-**B′** or [*S*,*S*]-**A** and [*S*,*R*]-**A′** (see Scheme 2) were located in which the *ansa*-ligand of [*S*]-**6** or [*S*]-**3b** adopts a 'C_2-symmetric' conformation with respect to the six-membered ring involving the metal, the aldehyde and the η^1-crotyl ligand. The overall geometry of the *ansa*-ligand is quite similar to that observed in the X-ray structure of *rac*-**5** or *rac*-**4** (e.g. Fig. 2(a)). A brief perusal of the results summarized in Table 6 reveals that [*S*,*S*]-**B** (or [*S*,*S*]-**A**) is usually higher in energy than [*S*,*R*]-**B′** (or [*S*,*R*]-**A′**) and on this basis one would predict that the [*R*] enantiomer of the anti-homoallylic alcohol would be favoured using either [*S*]-metallocene reagent; this is what is typically observed using [*S*]-**3b**.

However, another, lower energy conformer was located for the [*S*,*S*]-diastereomer arising from [*S*]-**6** ([*S*,*S*]-**B″**) in which the *ansa*-ligand adopts a skewed, asymmetric geometry with respect to the equatorial ligands [16]. In fact, the geometry adopted by the *ansa*-ligand in [*S*,*S*]-**B″** (Fig. 2(b)) is remarkably similar to that adopted in the X-ray structure of *rac*-**5** in the space group $P2_1/c$ [10a]; one of the t-butyl groups on the Cp rings almost bisects the angle defined by oxygen, titanium and the α-carbon of the crotyl ligand and other is located well off to the other side. For $PhCH_2CHO$, c-$C_6H_{11}CHO$ and PhCHO, [*S*,*S*]-**B″** is the lowest energy conformer by a significant amount, whereas for ^{t}BuCHO [*S*,*S*]-**B″** is still lowest in energy but by a reduced amount.

These findings should be interpreted with considerable caution; the magnitude of the calculated energy differences are not in agreement with the experimental

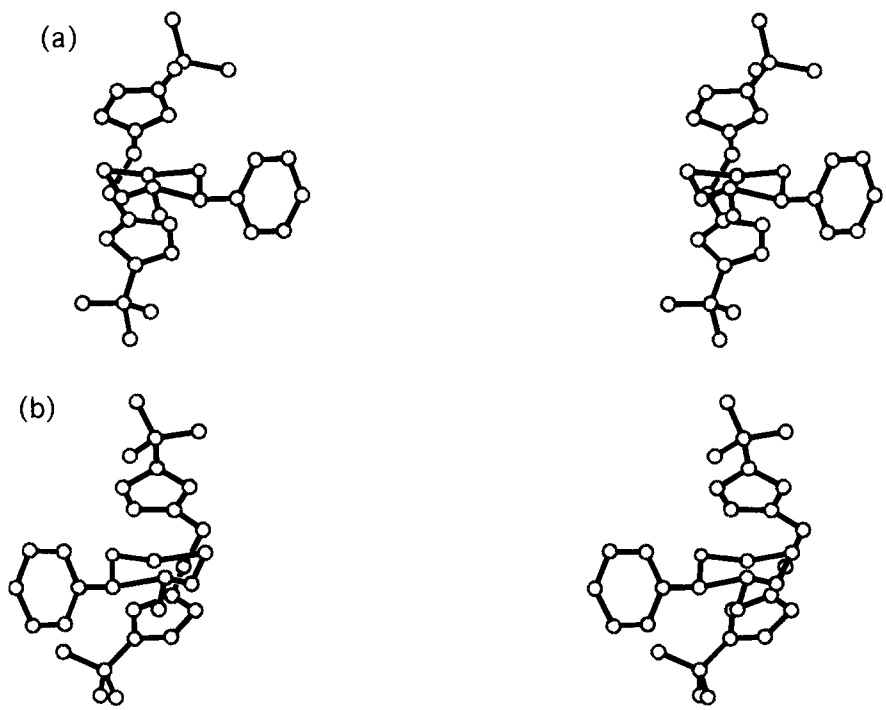

Fig. 2. Minimized structures for the interaction of [*S*]-**6** with benzaldehyde. Hydrogen atoms have been omitted for clarity: (a) [*S*,*R*]-**B′** diastereomer; (b) [*S*,*S*]-**B″** diastereomer (global minimum).

data, and, in the case of pivaldehyde, the observed reversal in selectivity using [*S*]-**6** is not borne out by the calculations. This is undoubtedly due to the simplistic approach adopted for parameter assignment to the atoms involved in the transition state and the crude, force field employed within PCMODEL for transition metal atoms. It is nonetheless interesting that these models predict opposite behaviour for [*S*]-**6** vs. [*S*]-**3b** with most aldehydes.

4. Conclusions

The reactions of [*S*]-**6** with aldehydes proceeds with variable diastereo- and enantio-selectivity and in moderate to good yield. The stereochemical results can be partially rationalized using fairly simple, molecular modelling calculations. The latter results suggest that the assumption of C_2 symmetry, which is frequently invoked to explain stereoselective reactions occurring at *ansa*-metallocenes related to [*S*]-**6**, may not always be valid, particularly for those systems which are conformationally flexible. This finding has been alluded to before in studies concerned with conformational properties of *ansa*-metallocenes [10b,17].

5. Experimental details

All reactions were performed under an atmosphere of argon or dry nitrogen. Standard techniques for the manipulation of air and moisture sensitive solids were employed [18]. All solvents were reagent grade that were obtained from commercial sources and purified by distillation as required. Tetrahydrofuran, diethyl ether, hexane and toluene were refluxed and distilled from sodium benzophenone ketyl under nitrogen. Crotylmagnesium chloride was prepared from crotyl chloride and magnesium metal in diethyl ether. Racemic binaphthol was resolved by the method of Kazlauskas [19]. [*S*]-O-acetylmandelic acid was prepared from [*S*]-mandelic acid by the literature procedure [20]. The optical purity of the homoallylic alcohols prepared was determined by HPLC analyses of the 3,5-dinitrobenzoylcarbamate derivatives on a chiral column as previously described [7]. Authentic samples of each homochiral alcohol were obtained using the methodology developed by Roush and co-workers [21].

Elemental analyses were performed by M-H-W Laboratories. ^{1}H and ^{13}C NMR spectra were recorded on Bruker AM 250 or AC 200 spectrometers. Optical rotations were performed on a JASCO DIP-360 digital polarimeter. HPLC analyses were performed on a Waters 600E instrument equipped with a Pirkle [22] column (covalent D-naphthylalanine, Regis Chemical), a Waters 484 UV-visible detector and a Waters 745 recording integrator.

5.1. Kinetic resolution of rac-5

To a suspension of finely divided sodium metal (ca. 0.5 g) in toluene (70 ml) at 80°C was added *rac*-**5** (0.3450 g, 0.89 mmol) and [*S*]-binaphthol (0.1294 g, 0.45 mmol, 99.5% ee) in one portion. The vigorously stirred suspension was monitored by TLC for the disappearance of binaphthol. The time for completion of the reaction varies depending on the particle size of the sodium metal; it is essential that the reaction be stopped when all the binaphthol has been consumed (typically < 30 min using finely divided sodium). Once the reaction was complete, the mixture was rapidly cooled in an ice bath and the excess sodium metal was removed by filtration through Celite and the solvent removed in vacuo.

The resulting red oil was chromatographed on silica gel, eluting with petroleum ether : toluene (5 : 1) to provide [*S,S*]-**7** (157 mg, 53% yield for one enantiomer). ^{1}H NMR (200 MHz, $CDCl_3$): δ 7.78 (t, $J = 8.6$ Hz, 4H), 7.22–6.88 (m, 8H), 6.02 (t, 2H), 5.80 (t, 2H), 5.19 (t, 2H), 3.44–3.13 (AA'BB' multiplet, 4H) 0.66 (s, 18H). ^{13}C NMR (50 MHz, $CDCl_3$): δ 182.63, 165.33, 156.38, 135.73, 134.95, 128.60, 127.46, 126.95, 125.12, 121.89, 121.03, 117.34, 112.63, 105.08, 33.41, 31.25, 30.09, 28.93. $[\alpha]_{577} = +5316°$ ($l = 10$ cm, $c = 4.9$ mg (100 ml)$^{-1}$, $CHCl_3$). Elemental Anal. Calc. for $C_{40}H_{40}O_2Ti$: C, 79.99 H, 6.71. Found: C, 80.23 H, 6.94.

A similar reaction with *rac*-**5** and *rac*-binaphthol (1 equiv.) provided *rac*-**7** in 53% yield. Crystals of *rac*-**7**, suitable for X-ray crystallography were grown by slow evaporation of a toluene/iso-octane solution. For crystallographic data see Tables 1–3.

5.2. Conversion of [S,S]-7 to [S]-5

Spectroscopically pure [*S,S*]-**7** (0.2027 g, 0.34 mmol) was dissolved in hexane (10 ml) and cooled to −78°C. An ether solution of methyllithium (2.4 ml of 1.4 M, 10 equiv.) was added via syringe and the reaction warmed to RT and stirred at RT overnight. The suspension was concentrated to ca. 5 ml and diluted with 10 ml of hexane, filtered under Ar and the filter cake washed with an additional 10 ml of hexane to free the yellow dimethyl compound, [*S*]-**8**, of excess MeLi and salts. The filtrate, which contains pure [*S*]-**8**, can be concentrated in vacuo to provide material for determination of e.g. optical purity, or can be directly converted to [*S*]-**5** by the following procedure:

A solution of anhydrous HCl in diethyl ether (ca. 2.0 M) was prepared by bubbling HCl gas into dry diethyl ether that was vigorously stirred over anhydrous $CaCl_2$. An excess (ca. 250 μl) of this solution was added to the hexane filtrate at 0°C to give a deep red solution. Spectroscopically pure [*S*]-**5** (0.1246 g, 0.32 mmol) was

isolated in 95% yield upon removal of the solvents in vacuo. Optical rotation $[\alpha]_{435} = -1663°$ (10 cm, c = 3.5 mg (100 ml)$^{-1}$, $CHCl_3$). Spectral data were identical with that reported for the racemate [10a]. Elemental Anal. Calc. for $C_{20}H_{28}Cl_2Ti$: C, 62.03, H, 7.29. Found: C, 62.36, H, 7.44.

5.3. Enantiomeric purity of [S]-8

A solution of [S]-O-acetylmandelic acid (19.4 mg, 0.1 mmol in 1.0 ml of $CDCl_3$) was added to a vial containing [S]-**8** (17.3 mg, 0.05 mmol) in a glove-box. Upon shaking, the colour of the solution changed from yellow to orange with vigorous evolution of methane. After 30 min, the solution was filtered through a plug of glass wool into a NMR tube and the ^{1}H NMR spectrum recorded. For ^{1}H NMR data for both diastereomers, see Table 4. In the case of the spectrum obtained from [S]-**8**, only the signals dues to [S,S,S]-**10** were present.

5.4. Preparation of [S]-6 and reaction with aldehydes

To a solution of [S]-**5** (0.947 g, 0.24 mmol) in hexane or THF (2.0 ml) was added 1.2 equiv. of solution of ^{n}PrMgCl in ether (330 μl, 0.89 M). The colour of the solution changed to green black, and, in the case of hexane, a precipitate was observed on the walls of the reaction flask. The mixture was briefly heated to reflux, using a heat-gun, and then cooled to room temperature. After 15 min, 0.9 equiv. of a solution of crotylMgCl in ether (183 μl, 1.2 M) was added. The violet solution was stirred at RT for 1 h. The aldehyde (0.29 mmol) was then added neat, via syringe and the reaction mixture kept at RT for 1.5 h, before being quenched with HCl in Et_2O. After drying over Na_2SO_4, filtration and removal of the solvents in vacuo, the homoallylic alcohol products were purified by flash chromatography on silica gel eluting with 2 : 1 petroleum ether : toluene (to recover [S]-**5**) and then 9 : 1 hexanes : EtOAc. For spectral data and procedures for the HPLC analyses of the products, see Ref. [7].

Acknowledgements

The authors wish to thank the Natural Sciences and Engineering Research Council of Canada for financial support of this work.

References and notes

[1] (a) W.R. Roush, in C.H. Heathcock (ed.) *Comprehensive Organic Synthesis*, Pergamon, New York, 1991, Vol. 2, pp. 1–54; (b) Y. Yamamoto, *Acc. Chem. Res., 20* (1987) 243; (c) R.W. Hoffmann, *Angew. Chem., Int. Ed. Engl., 26* (1987) 489.

[2] S.E. Denmark and E.J. Weber, *Helv. Chim. Acta, 66* (1983) 1655.

[3] (a) H.A. Martin and F. Jellinek, *J. Organomet. Chem., 12* (1968) 149; (b) H.A. Martin and F. Jellinek, *J. Organomet. Chem., 8* (1967) 115; (c) H.A. Martin and F. Jellinek, *J. Organomet. Chem., 6* (1966) 293.

[4] (a) Y. Kobayashi, K. Umeyama and F. Sato, *J. Chem. Soc., Chem. Commun.*, (1984) 621; (b) F. Sato, H. Uchiyama, K. Iida, Y. Kobayashi and M. Sato, *J. Chem. Soc., Chem. Commun.*, (1983) 921; (c) F. Sato, Y. Suzuki and M. Sato, *Tetrahedron Lett., 23* (1982) 4589; (d) F. Sato, S. Iijima and M. Sato, *Tetrahedron Lett., 22* (1981) 243.

[5] S. Collins, W.P. Dean and D.G. Ward, *Organometallics, 7* (1988) 2289.

[6] F. Sato, S. Iijima and M. Sato, *J. Chem. Soc., Chem. Commun.*, (1981) 180.

[7] S. Collins, B.A. Kuntz and Y. Hong, *J. Org. Chem., 54* (1989) 4154.

[8] For much improved results using cyclopentadienyltitanium(IV) allyl complexes see (a) R.O. Duthaler and A. Hafner, *Chem. Rev., 92* (1992) 807; (b) A. Hafner, R.O. Duthaler, R. Marti, G. Rihs, P. Rothe-Streit and F. Schwarzenbach, *J. Am. Chem. Soc., 114* (1992) 2321; (c) M. Reidiker and R.O. Duthaler, *Angew. Chem., Int. Ed. Engl., 28* (1989) 494. See also (d) M.T. Reetz, S.H. Kyung and J. Westermann, *Organometallics, 3* (1984) 1716.

[9] (a) A. Schafer, K. Eberhard, L. Zsolnai, G. Huttner and H.-H. Brintzinger, *J. Organomet. Chem., 328* (1987) 87; (b) F.W.R.P. Wild, L. Zsolnai, G. Huttner and H.-H. Brintzinger, *J. Organomet. Chem., 232* (1982) 233.

[10] (a) S. Collins, Y. Hong and N.J. Taylor, *Organometallics, 9* (1990) 2695; (b) S. Collins, Y. Hong, R. Ramachandran and N.J. Taylor, *Organometallics, 10* (1991) 2349.

[11] A. Dorigo and K.N. Houk, *Adv. Mol. Model., 1* (1988) 135.

[12] (a) F.M. Menger and M.J. Sherrod, *J. Am. Chem. Soc., 112* (1990) 8071; (b) M.J. Sherrod and F.M. Menger, *J. Am. Chem. Soc., 111* (1989) 2611.

[13] F. Jensen, *J. Am. Chem. Soc., 114* (1992) 1596.

[14] Standard parameters using the MMX force field contained with the program PCMODEL (Version 3.0, Serena Software) were employed throughout. Although the absolute values of the MMX energies varied enormously, the basic conclusions of these studies are not dramatically affected by parameter selection for the atoms in these structures. This is probably a reflection of both the mediocre treatment of transition metal atoms using the default MMX force-field contained with PCMODEL and the generally excellent treatment of steric effects with which the present study is concerned.

[15] The boat-like 'transition' states leading to the syn diastereomers were also examined and their relative energies were consistent with the experimental results observed using e.g. $PhCH_2CHO$. The energies of the less stable, boat-like transition states compared with the chair transition states were highly dependent on the value of the bond order between the C=O carbon and the γ-carbon of the crotyl ligand; high bond orders accentuated the energy differences, as might be expected. Furthermore, a single value for this parameter could not be obtained that led to uniform agreement between calculated and experimental values for the simple diastereoselectivity of these reactions.

[16] A conformer of the [S,R]-diastereomer, analogous to that of [S,S]-**B''**, was located but, this was higher in energy than those summarized in Table 6 (asymmetric conformers derived from [S]-**3b** were also studied but, were much higher in energy than C_2 symmetric analogues). Also, conformers in which the ansa-ligand adopted the [S]-λ conformation were examined; these were usually higher in energy and, in any event, did not change the relative ordering of the two diastereomeric transition states.

[17] P. Burger, J. Diebold, S. Gutmann, H.-U. Hund and H.-H. Brintzinger, *Organometallics, 11* (1992) 1319.
[18] D.F. Shriver and M.A. Drezdon, *Manipulation of Air-sensitive Compounds,* 2nd edn., Wiley, New York, 1986.
[19] R.J. Kazlauskas, *Org. Syn., 70* (1991) 60.
[20] E.G. Breitholle and C.H. Stammer, *J. Org. Chem., 39* (1974) 1311.
[21] W.R. Roush and R.L. Halterman, *J. Am. Chem. Soc., 108* (1986) 294.
[22] (a) W.H. Pirkle and T.C. Pochapsky, *Chem. Rev.,* 89 (1989) 347; (b) W.H. Pirkle, T.C. Pochapsky, G.S. Mahler, D.E. Corey, D.S. Reno and D.M. Alessi, *J. Org. Chem., 51* (1986) 4991; (c) W.H. Pirkle, G.S. Mahler and M.H. Hyun, *J. Liq. Chromatogr., 9* (1986) 443.